

Synthesis of TiN, VN, and CrN from Ammonolysis of TiS_2 , VS_2 , and Cr_2S_3 ¹

P. Subramanya Herle,* M. S. Hegde*,² N. Y. Vasathacharya*, and Sam Philip†

*Solid State and Structural Chemistry Unit, †Materials Research Center, Indian Institute of Science, Bangalore 560012, India

and

M. V. Rama Rao and T. Sripathi

Inter University Consortium, Indore 452001, India

Received February 28, 1997; in revised form July 7, 1997; accepted July 15, 1997

A new route to synthesize pure TiN, VN, and CrN from the ammonolysis of TiS_2 , VS_2 , and Cr_2S_3 is described. Thermogravimetric analysis and temperature-programmed reaction (TPR) of TiS_2 , VS_2 , and Cr_2S_3 with ammonia are employed to understand the reaction pathway to nitride formation. X-ray photoelectron spectroscopic studies confirm the formation of pure nitride phases. Reactivity of these nitride powder toward oxidation was examined by TPR studies. Magnetic susceptibility measurements show that TiN is Pauli-paramagnetic and VN is weakly paramagnetic, whereas CrN shows a paramagnetic to antiferromagnetic transition at 280 K. Electrical conductivity measurements show TiN and VN are metallic, whereas CrN is semiconducting. © 1997 Academic Press

New synthetic routes to nitrides of both transition metals and main-group elements are of current interest due to their technological importance (1–3). Nitrides have a small free energy of formation due to the strong $N\equiv N$ bond in dinitrogen. Therefore the synthesis of nitrides in general is more difficult than the synthesis of oxides. Nitrogen-rich phases of transition metal nitrides are not stable at high temperatures, and therefore new low-temperature synthetic routes are becoming important (4). Binary and ternary nitrides such as MoN (5), VN (6), $LiMoN_2$ (7), and $LiWN_2$ (8) have been synthesized by ammonolysis of the corresponding oxide precursors. Direct decomposition of molecular precursors is an attractive method to obtain new nitride phases (9). Decomposition of metal amides in a nitrogen atmosphere is yet another route to nitrides (10). Reaction of alkali metal nitrides with metal halides has given rise to new nitride phases (11). Heating metal powder with alkali or alkaline

earth metal nitrides in a nitrogen atmosphere has also given new nitride phases (12). Reaction of sulfides with ammonia could also give nitrides which has not yet been explored except for the reaction of P_4S_{10} with ammonia to give P_3N_5 (3) and molybdenum nitride phases form MoS_2 (13). In this paper, we report the first synthesis of TiN, VN, and CrN by ammonolysis of TiS_2 , VS_2 , and Cr_2S_3 .

EXPERIMENTAL

Pure (99.8%) TiS_2 , VS_2 , and Cr_2S_3 from Alpha Chemicals were used in this study. In a typical experiment, ≈ 30 mg of TiS_2 was loaded in a homebuilt thermogravimetric analyzer (TGA), and the weight loss was measured in flowing NH_3 gas as a function of temperature up to $800^\circ C$ with a heating rate of $3^\circ C\ min^{-1}$. The sample was heated isothermally at $800^\circ C$ till the reaction was complete, and the sample was cooled in an NH_3 atmosphere to room temperature. The sample was reheated in an O_2 atmosphere to estimate the nitrogen content. Similar experiments were carried out using VS_2 and Cr_2S_3 as starting materials. TPR of the sulfides was carried out employing a homebuilt apparatus (14). In a typical experiment, 200 mg of the sulphide was loaded and the reactor was evacuated to 10^{-6} Torr. Ammonia gas was admitted at about $15\text{--}20\ \mu\text{mol s}^{-1}$ and the reactor was heated from 30 to $750^\circ C$ at a rate of $15^\circ C\ min^{-1}$. The gaseous products were analyzed by a VG QXK300 quadrupole mass spectrometer. Bulk samples were synthesized by heating ≈ 2.5 g of sulfide in an alumina boat in a quartz tube under flowing ammonia gas (flow rate $\approx 120\ \text{ml min}^{-1}$) and then cooled to room temperature in an ammonia atmosphere at $5^\circ C\ min^{-1}$. The samples were analyzed for phase purity and structure by powder X-ray diffraction employing a JEOL8P powder diffractometer ($CuK\alpha$ radiation). EDX analysis of these samples was

¹ Contribution 1262 from the Solid State and Structural Chemistry Unit.

² To whom correspondence should be addressed.

carried out using a Cambridge S-360 scanning electron microscope (SEM) with a link Systems AN10000 X-ray analyzer to determine if there were any sulfur impurity. Nitrogen estimation was also carried out by heating 0.2 g of the nitride in dry NaOH at 800°C for 2 h in a pure argon atmosphere and liberated ammonia was estimated (15). The surface area of TiN was measured using a Micromeritics 2200 rapid surface area analyzer. X-ray photoelectron spectra were recorded in a VSW instrument. The magnetic susceptibility of these samples was studied using a Lewis coil force magnetometer, and electrical properties were measured using a pressed pellet employing the four-probe technique.

RESULTS AND DISCUSSION

In Fig. 1, the TGA curve of the ammonolysis of TiS_2 is given. The weight loss of 45.1% versus the expected value of 44.7% is an indication of complete conversion of TiS_2 to TiN. In the inset, the TGA of oxidation of titanium nitride in an oxygen atmosphere is shown. The mass gain of 29.4% is near the theoretical value of 29.06% for the oxidation of TiN to TiO_2 , confirming stoichiometric TiN. Similar experiments were carried out with VS_2 and Cr_2S_3 , and the results are summarized in Table 1. To determine the gaseous products of the reaction between sulfide and ammonia, a TPR experiment was carried out. The TPR of the ammonolysis of TiS_2 gave the gaseous products H_2S , N_2 , and H_2 , and the typical reaction profile is shown in Fig. 2. Liberated H_2S was reduced to sulfur as seen from the deposition of sulfur in the cooler part of the quartz tube. Whereas the intensity of N_2 reached a plateau, the intensity of H_2S first increased and then started decreasing, indicating decomposition of H_2S .

Bulk TiN was synthesized by heating TiS_2 under pure ammonia (flow rate $\approx 120 \text{ ml min}^{-1}$) in a quartz tube at 750°C. After several experiments, we found that 750°C is the optimum temperature with a reaction duration of 12 h. Here also, sulfur deposition was observed in the cooler region of the quartz tube. The sample was cooled and the dark brown product was analyzed. TPR of VS_2 with ammonia gave N_2 , H_2S , and H_2 at 475°C, whereas TPR of Cr_2S_3 with ammonia gave the same gaseous products at 425°C. VS_2 and

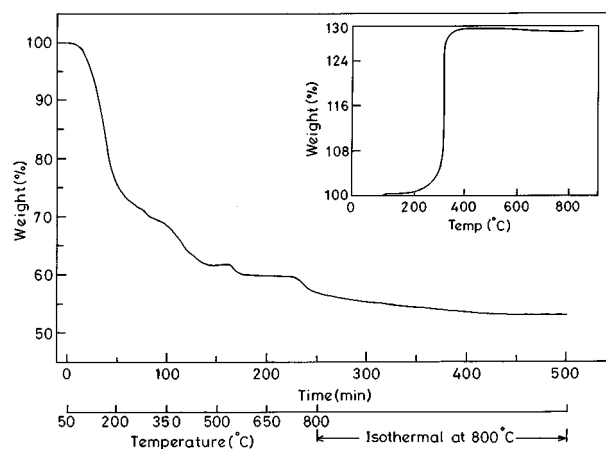


FIG. 1. TGA of TiS_2 in flowing NH_3 gas (heating rate 3°C min^{-1}). Inset shows oxidation of TiN in O_2 .

Cr_2S_3 were heated in ammonia at 725°C for 12 h to obtain bulk VN and CrN. VN was red-brown whereas CrN was gray-brown.

Powder X-ray diffraction patterns of TiN, VN, and CrN are shown in Figs. 3a–c respectively, and it is clear from the patterns that there are no impurity phases. The lattice parameter $a = 4.241(2) \text{ \AA}$ for TiN, $4.140(2) \text{ \AA}$ for VN, and $4.148(3) \text{ \AA}$ for CrN obtained here agrees well with the values reported in the literature (16). The powder X-ray diffraction patterns of these samples show that the lines are broader, indicative of small particle size. EDX analysis of all three samples did not show sulfur impurity peaks, confirming sulfur-free nitride phases. The surface morphologies of TiN, VN, and CrN are shown in Figs. 4a–c, respectively. It is clear from the figures that the particles are small, on the order of $0.5 \mu\text{m}$. The particle sizes of CrN and TiN are in the same regime, whereas VN has a smaller size. The surface area of TiN was measured employing a surface area analyzer and found to be $35 \text{ m}^2 \text{ g}^{-1}$, which is reasonably high. The nitrogen contents of the TiN, VN, and CrN phases were independently determined by chemical analysis and the compositions agree well with the TGA results. The results are summarized in Table 1.

TPR of a freshly prepared TiN sample in an oxygen atmosphere gave TiO_2 and N_2 as shown in Fig. 5a. No SO_2

TABLE 1
Synthesis and Characterization of TiN, VN, and CrN

Compound	Ammonolysis conditions	wt % N		Color	Electrical property	Magnetic property
		TGA	Chemical analysis			
TiN	750°C, 12 h	22.27 (2)	22.09 (2)	Dark brown	Metallic	Pauli-paramagnetic
VN	725°C, 12 h	21.22 (2)	20.71 (2)	Red-brown	Metallic	Paramagnetic
CrN	725°C, 12 h	20.54 (2)	20.20 (2)	Gray-brown	Semiconducting	Antiferromagnetic below 280 K

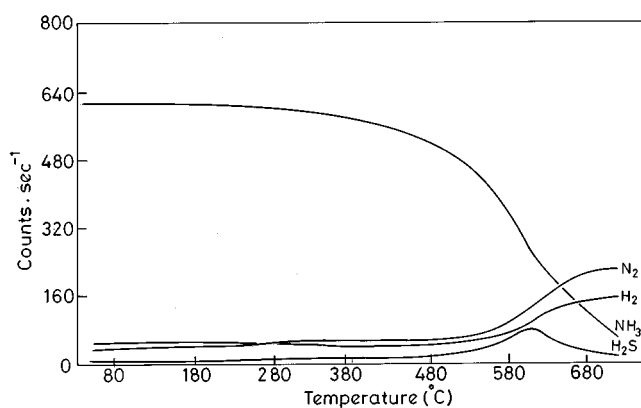
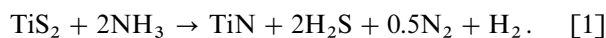


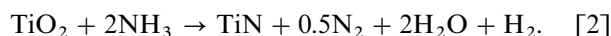
FIG. 2. Temperature-programmed reaction profile for the ammonolysis of TiS_2 .

or any other sulfur product could be detected in the mass spectrometer, indicating that the nitride is free from sulfur. TPR of VN and of CrN in oxygen are shown in Figs. 5b and 5c, respectively. The oxidation of VN to V_2O_5 occurred between 250 and 420°C. In the case of CrN, the reaction started at 400°C and was complete at 650°C. The oxidized products of TiN, VN, and CrN were analyzed and found to be TiO_2 , V_2O_5 , and Cr_2O_3 , respectively. It is interesting to note that oxidation of these nitride powders did not give any oxides of nitrogen.

From the TPR studies, we can write the chemical equation for the ammonolysis of TiS_2 as



The gaseous product H_2S is reduced to elemental sulfur. The free energy change, ΔG , as a function of temperature for the above reaction was calculated using the reported thermochemical data (17) and is given in Fig. 6a. From this figure, it is clear that above 550 K, ΔG is negative, supporting the feasibility of the reaction. A comparison was made with the ammonolysis of TiO_2 . In Fig. 6b we show ΔG as a function of temperature for the reaction



It is clear that ΔG is negative for the conversion of TiO_2 to TiN at a relatively high temperature (1000 K), indicating the advantage of conversion of TiS_2 to TiN. We studied the ammonolysis of TiO_2 ; the gaseous products were N_2 , H_2 , and H_2O , emanating above 725°C, which confirmed the prediction.

In the reaction of TiS_2 and VS_2 with ammonia to form TiN and VN, the oxidation states of the metal ions are reduced from +4 to +3. In the case of the conversion of Cr_2S_3 to CrN, there is no change in the formal oxidation state of the metal ion. Conversion of Cr_2O_3 to CrN is not feasible as ΔG is positive even up to 1300 K. Therefore, Cr_2S_3 to CrN conversion by ammonolysis is a new reaction and understanding the mechanism of conversion requires further studies. Since thermochemical data of Cr_2S_3 and VS_2 are not available, we could not calculate ΔG for reactions similar to Eq. [1].

To elucidate the electronic structure of these nitrides, X-ray photoelectron spectroscopic studies were done on the freshly prepared powder samples. In all three samples, S(2p)

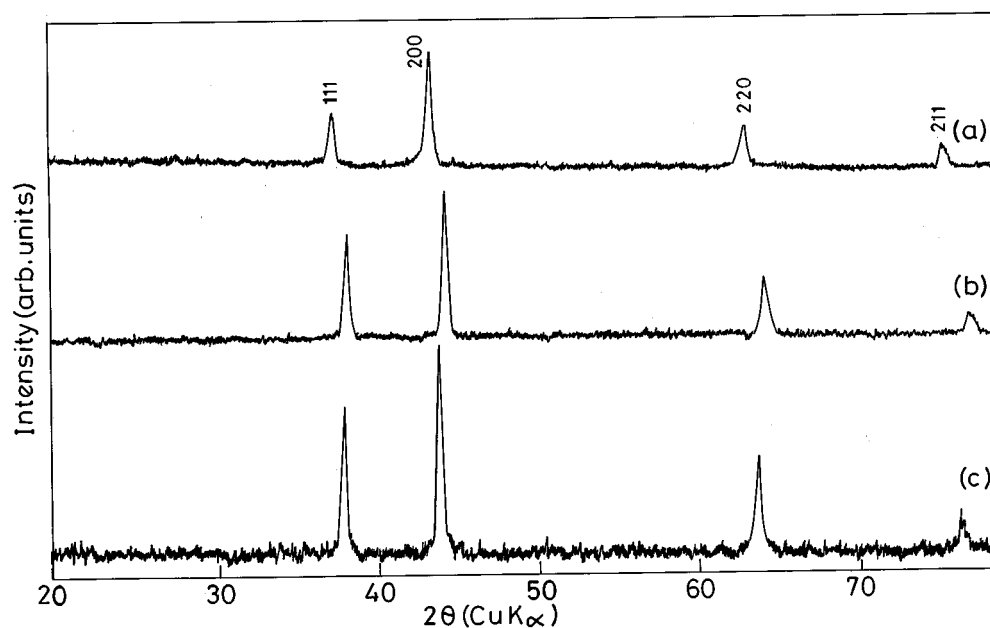


FIG. 3. Powder X-ray diffraction patterns of (a) TiN, (b) VN, and (c) CrN.

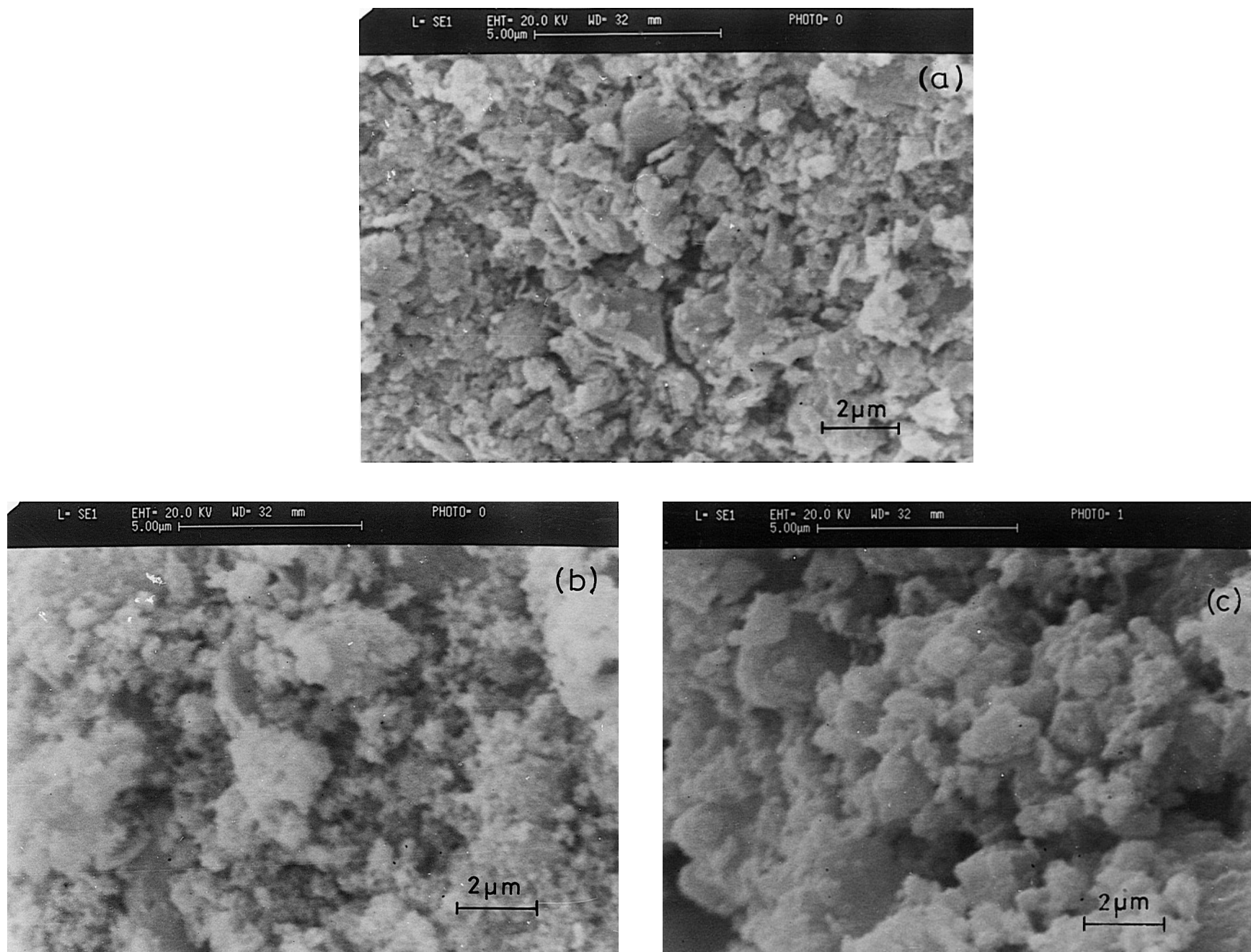


FIG. 4. SEM pictures of (a) TiN, (b) VN, and (c) CrN.

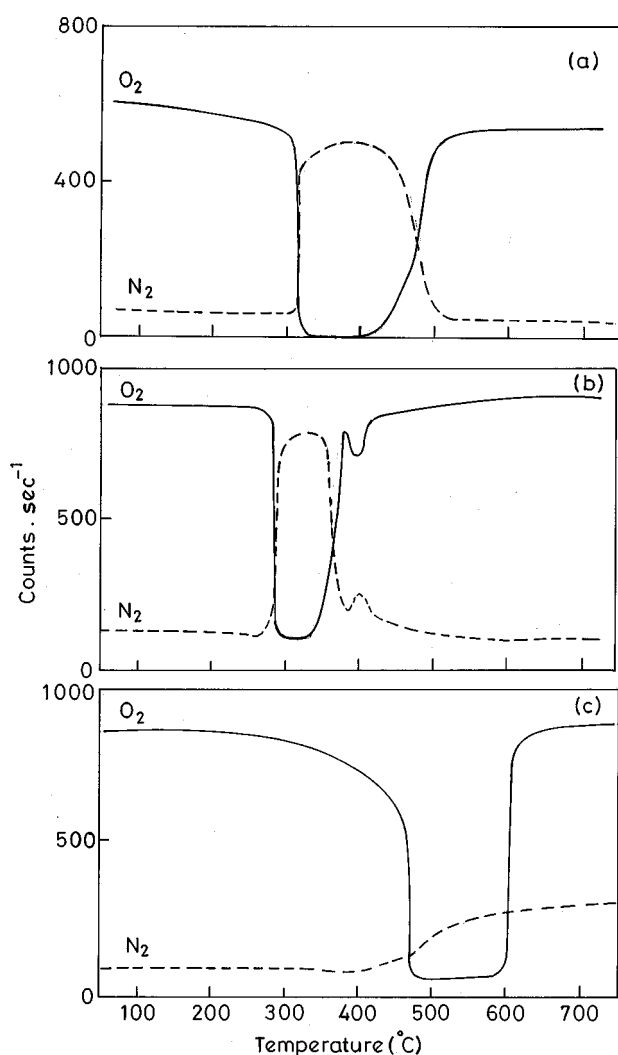


FIG. 5. TPR for the oxidation of (a) TiN, (b) VN, and (c) CrN.

and S(3s) core-level peaks were absent, further confirming complete conversion of sulfide to nitride. Core-level binding energies of metal 2p and N(1s) from TiN, VN, and CrN are summarized in Table 2. Ti(2p) and N(1s) binding energies agree well with the values reported in the literature (18). The binding energy of $V^{3+}(2p_{3/2})$ in VN at 513.7 eV is lower than that of $V^{3+}(2p_{3/2})$ in V_2O_3 at 515 eV (19), and higher than that of $V^0(2p_{3/2})$ in vanadium metal at 512.1 eV (20). The binding energy of $Cr^{3+}(2p_{3/2})$ in CrN at 575.5 eV is also lower than that of Cr^{3+} in Cr_2O_3 at 576.3 eV. The N(1s) bands of TiN, VN, and CrN are shown in Fig. 7a. XPS of Cr(2p) is shown in Fig. 7b. N(1s) showed a decrease in binding energy from 396.6 eV in TiN to 396.1 eV in CrN, indicating an increase of ionic character from TiN to CrN. XPS of the Cr(3s) region is shown in Fig. 8. The Cr(3s) peak is split into two peaks which are separated by 4.1 eV. This is to be attributed to exchange splitting due to three unpaired

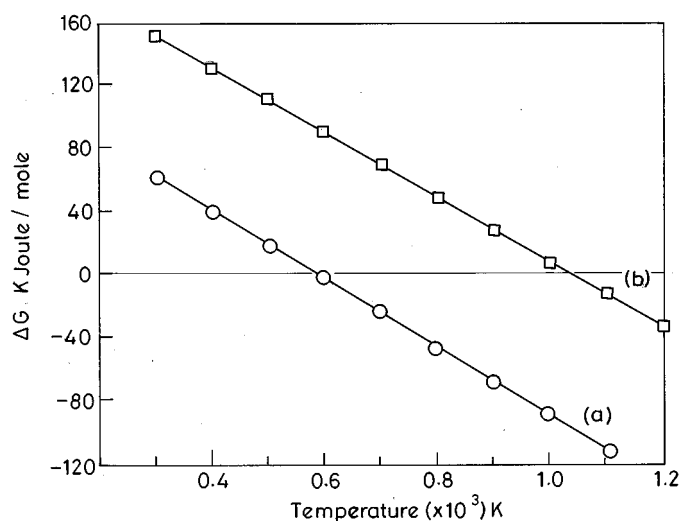


FIG. 6. ΔG vs temperature plot for the conversion of (a) TiS_2 to TiN and (b) TiO_2 to TiN.

electrons in $Cr^{3+}(3d)$ of CrN. The exchange splitting of 4.1 eV in CrN is lower than that of 4.4 eV in Cr_2O_3 (19). Therefore both the core-level binding energies of metal 2p and the exchange splitting demonstrate that the nitrides are more covalent than the corresponding trivalent metal oxides. The valence-band region of CrN is also shown in Fig. 8. The spectrum shows $Cr^{3+}(3d)$ and $N^{3-}(2p)$ bands. The $N^{3-}(2p)$ band at 5.1 eV in CrN is close to that of $N^{3-}(2p)$ in TiN. In the case of TiN, a sharp increase in electron emission observed at E_F is indicative of metallic behavior (18). However, a much smaller intensity of electron emission at E_F (Fig. 8) is observed in the case of CrN, and the 3d band moved towards the N(2p) band. This is a clear indication of the semiconducting nature of CrN.

Magnetic susceptibilities of TiN, VN, and CrN as a function of temperature are shown in Figs. 9a–c respectively. TiN showed Pauli-paramagnetic behavior down to 50 K, and below this temperature, an increase in susceptibility was observed. However, the increase in susceptibility value of 1.35×10^{-6} emu g^{-1} at 20 K from 0.5×10^{-6} emu g^{-1} at 300 K is very small, probably due to an impurity which

TABLE 2
Core-Level Binding Energies^a of TiN, VN, and CrN

Compound	$M(2p_{3/2})$	$M(2p_{1/2})$	N(1s)
TiN	456.0	461.5	396.6
VN	513.7	521.3	396.4
CrN	575.5	584.7	396.1

^a The values are with reference to C(1s) at 285 eV and they are accurate within ± 0.2 eV.

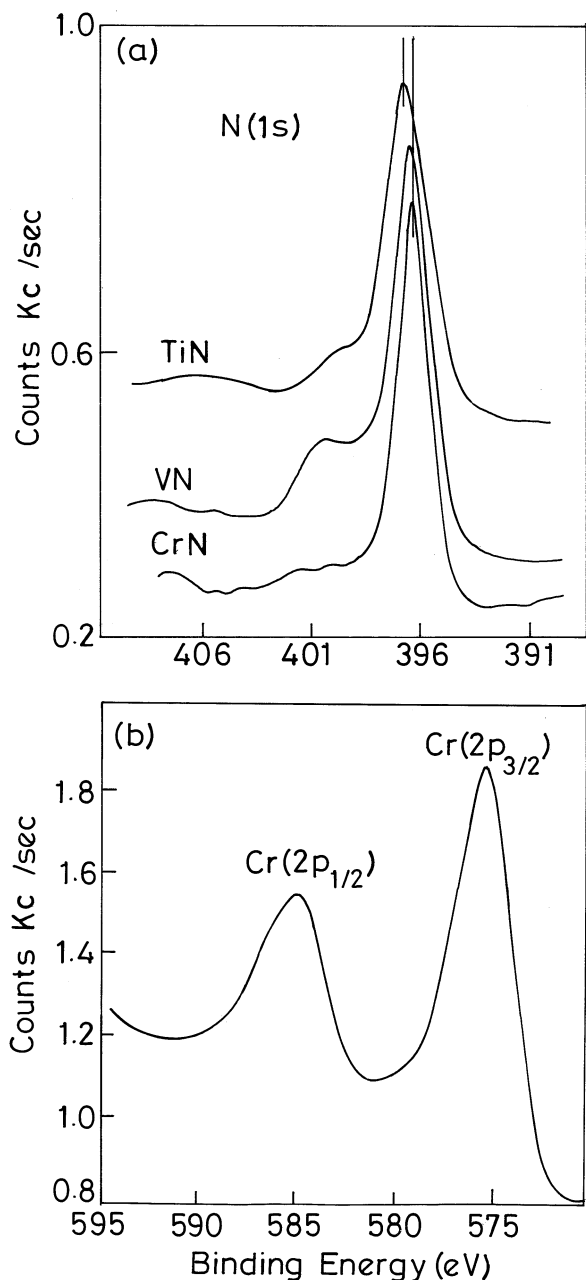


FIG. 7. XPS of (a) the N(1s) bands of TiN, VN, and CrN and (b) Cr(2p) of CrN.

could not be detected. In the case of VN, the room temperature susceptibility of $10 \times 10^{-6} \text{ emu g}^{-1}$ is indicative of the paramagnetic nature of the sample but, variation of χ vs T does not follow Curie law. CrN showed a paramagnetic to antiferromagnetic transition at 280 K. This result confirmed an earlier observation on CrN synthesized by other methods (21). There is no literature data on the magnetic susceptibility of CrN below 77 K. In our study, the χ vs T

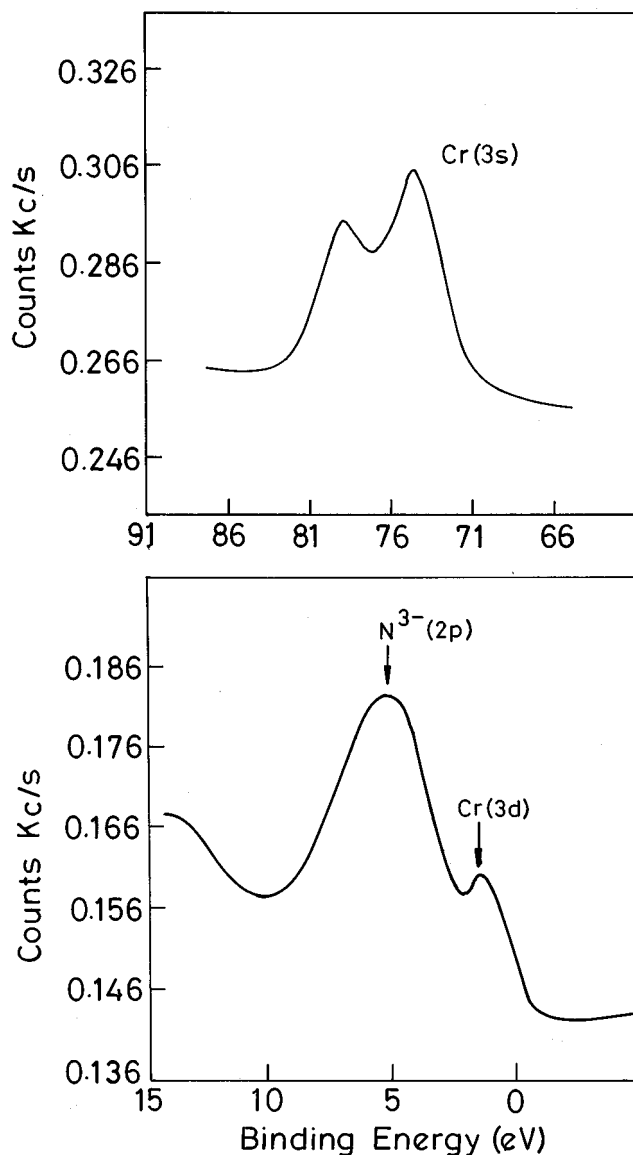


FIG. 8. XPS of Cr(3s) and the valence-band region of CrN.

plot showed a cusp at 47 K but the exact reason for such a behavior is not clear to us.

Resistivity vs temperature plots of TiN, VN, and CrN are shown in Figs. 10a–c, respectively. In the case of TiN and VN, there is no significant change in the resistivity with decreasing temperature, possibly due to grain boundary effects in the pressed pellet. The resistivity vs temperature behavior is indicative of the semiconducting nature of CrN. This is in conformance with the low density of states at E_F in the valence band of CrN. The plot of $\ln(\rho)$ vs $1/T$ did not give a straight line in the range $20 \leq T \leq 300 \text{ K}$. However, the plot of the $\ln(\rho)$ vs $1/T$ between 100 and 300 K gave a straight line and the band gap calculated from the slope of the curve is 0.09 eV.

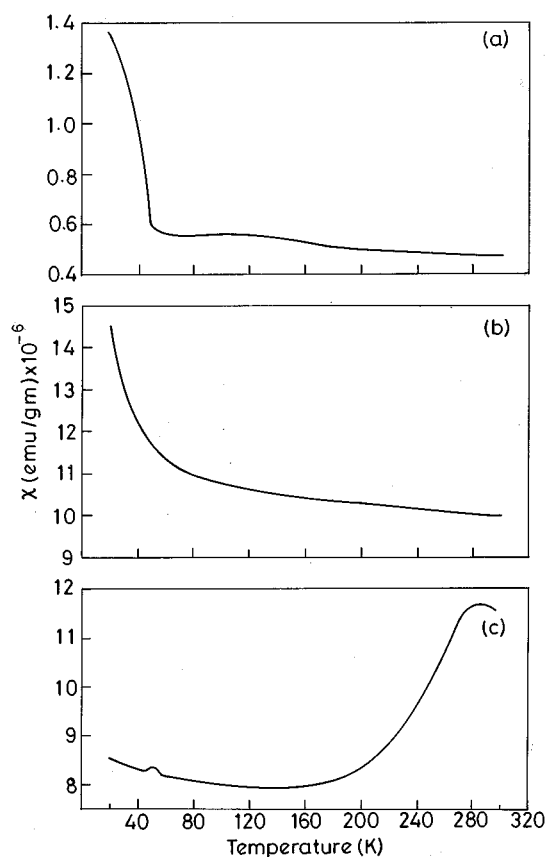


FIG. 9. χ vs T plot for (a) TiN, (b) VN, and (c) CrN.

Extension of this method for the synthesis of other binary nitrides was attempted. Direct reaction of NH_3 with commercial MoS_2 was sluggish and gave a mixture of different molybdenum nitride phases at different temperatures as reported in the literature (13). Since thermal decomposition of $(\text{NH}_4)_2\text{MoS}_4$ and $(\text{NH}_4)_2\text{WS}_4$ gives amorphous disulfides via trisulfide intermediates below 400°C (22), nitridation of amorphous disulfide will naturally be faster as compared to the corresponding disulfide crystalline samples. We have attempted to synthesize molybdenum and tungsten nitrides from the ammonolysis of the corresponding ammonium thio precursors. $(\text{NH}_4)_2\text{MoS}_4$ and $(\text{NH}_4)_2\text{WS}_4$ were synthesized by passing H_2S at 60°C through a solution of ammonium paramolybdate and ammonium paratungstate in aqueous ammonia (22). Ammonolysis of $(\text{NH}_4)_2\text{MoS}_4$ at 750°C for 12 h gave mixed phases containing MoN, Mo_2N , and MoS_2 . On further heating with ammonia at 750°C for 12 h, a decrease in MoS_2 and an increase in Mo_2N were observed. However, the final product was a mixture of Mo_2N and a small quantity of MoN. From a thermodynamic point of view, conversion of MoS_2 to Mo_2N or MoN as in Eq. [1] is not feasible as ΔG is positive even up to 1300 K, indicating a different type of

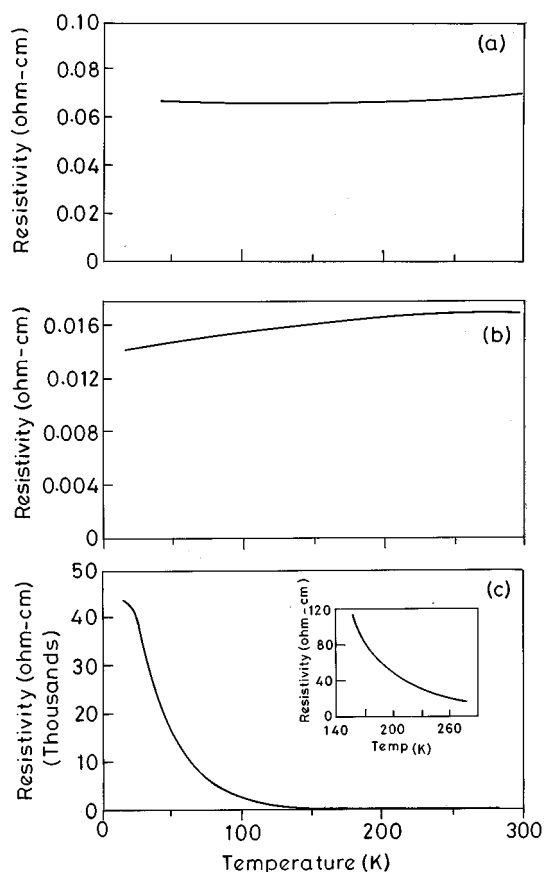


FIG. 10. ρ vs T plot for (a) TiN; (b) VN, and (c) CrN. Inset in (c) shows ρ vs T plot for the $140 \leq T \leq 300$ K range.

mechanism is operating in this reaction. Probably, MoS_2 was reduced to fine metal particles of molybdenum metal and subsequent reaction of metal particles with ammonia gave Mo_2N and MoN phases.

Surprisingly, ammonolysis of $(\text{NH}_4)_2\text{WS}_4$ at 750°C for 24 h yielded only a WS_2 phase. When heated further in ammonia at 800°C for 15 h, the tungsten sulfide was completely reduced to tungsten metal.

CONCLUSIONS

In conclusion, we have shown that pure TiN, VN, and CrN can be synthesized by the reaction of NH_3 with TiS_2 , VS_2 , and Cr_2S_3 , respectively. The nitride powders oxidized in an oxygen atmosphere show that CrN is stable up to 400°C , whereas TiN and VN are stable only up to about 250°C . Core-level binding energies of $M(2p)$ and $\text{N}(1s)$ from X-ray photoelectron spectroscopic studies showed that these nitrides are more covalent than the corresponding trivalent metal oxides. Magnetic susceptibility studies showed that TiN is Pauli-paramagnetic, VN is weakly paramagnetic, and CrN undergoes a paramagnetic

to antiferromagnetic transition below 28 K. Electrical measurement shows that TiN and VN are metallic whereas CrN is semiconducting. Ammonolysis of ammonium thiomolybdate gives a mixture of Mo₂N and MoN, whereas the ammonium thiotungstate gives only WS₂ or tungsten metal.

ACKNOWLEDGMENT

One of the authors (P. S. Herle) thanks the Council of Scientific and Industrial Research, New Delhi, for the award of a fellowship.

REFERENCES

1. L. E. Toth, "Transition Metal Carbides, and Nitrides." Academic Press, New York, 1971.
2. F. J. DiSalvo, *Science* **649**, 247 (1990).
3. W. Schnick, *Angew. Chem. Int. Ed. Engl.* **32**, 806 (1993).
4. S. H. Elder, F. J. DiSalvo, L. Topor, and A. Navrotsky, *Chem. Mater.* **5**, 1545 (1993).
5. C. N. Jagers, J. M. Michaels, and A. M. Stacy, *Chem. Mater.* **2**, 150 (1990).
6. R. Kapoor and S. T. Oyama, *J. Solid State Chem.* **99**, 303 (1992).
7. S. H. Elder, L. H. Doerrer, F. J. DiSalvo, J. B. Parise, D. Guyomard, and J. M. Tarascon, *Chem. Mater.* **4**, 928 (1992).
8. P. S. Herle, M. S. Hegde, N. Y. Vasathacharya, J. Gopalakrishnan, and G. N. Subbanna, *J. Solid State Chem.* **112**, 208 (1994).
9. H. P. Baldus, W. Schnick, J. Lücke, U. Wannagat, and G. Bogedain, *Chem. Mater.* **5**, 845 (1993).
10. A. P. Purdy, *Inorg. Chem.* **33**, 282 (1994).
11. E. G. Gillan and R. B. Kaner, *Inorg. Chem.* **33**, 5693 (1994).
12. A. Gudat, R. Knip, and J. Maier, *J. Alloys Compd.* **186**, 339 (1992).
13. R. J. Marchand, X. Gouin, F. Tessier, and Y. Laurent, *Mater. Res. Symp. Proc.* **368**, 15 (1995).
14. M. S. Hegde, S. Ramesh, and G. S. Ramesh, *Proc. Indian Acad. Sci., Chem. Sci.* **104**, 591 (1992).
15. T. L. Chu, C. H. Lee, and G. A. Gurber, *J. Electrochem. Soc.* **114**, 717 (1967).
16. Powder Diffraction File, 38-1840 for TiN, 35-768 for VN, and 11-65 for CrN. JCPDS International Center of Diffraction Data, Swathmore, PA.
17. O. Knache, O. Kubaschewski, and K. Hesselmann, (Eds.), "Thermochemical Properties of Inorganic Substances," 2nd ed. Springer-Verlag, Berlin, 1991.
18. S. V. Didziulis, J. R. Lince, T. B. Stewart, and E. A. Eklund, *Inorg. Chem.* **33**, 1979 (1994).
19. C. N. R. Rao, D. D. Sarma, S. Vasudevan, and M. S. Hegde, *Proc. R. Soc. London A* **367**, 239 (1979).
20. "Practical Surface Analysis by Auger and X-ray Photoelectron Spectroscopy" (D. Briggs and M. P. Seath, Eds.), p. 493. Wiley, New York, 1983.
21. L. M. Corliss, N. Elliott, and J. M. Hastings, *Phys. Rev.* **117**, 929 (1960).
22. T. P. Prasad, E. Diemann, and A. Müller, *J. Inorg. Nucl. Chem.* **35**, 1895 (1973).